Ab initio study of the electronic structure and elastic properties of Al_5C_3N*

Xu Xue-Wen(徐学文), Hu Long(胡 龙), Yu Xiao(宇 霄), Lu Zun-Ming(卢遵铭), Fan Ying(范 英), Li Yang-Xian(李养贤), and Tang Cheng-Chun(唐成春)†

School of Materials Science and Engineering, Hebei University of Technology, Tianjin 300130, *China*

(Received 4 March 2011; revised manuscript received 22 July 2011)

We investigate the electronic structure, chemical bonding and elastic properties of the hexagonal aluminum carbonitride, Al_5C_3N, by *ab initio* calculations. Al_5C_3N is a semiconductor with a narrow indirect gap of 0.81 eV. The valence bands below the Fermi level (E_F) originate from the hybridized Al p–C p and Al p–N p states. The calculated bulk and Young's moduli are 201 GPa and 292 GPa, which are slightly lower than those of Ti_3SiC_2. The values of the bulk-to-shear-modulus and bulk-modulus-to-c_{44} are 1.73 and 1.97, respectively, which are higher than those of Ti_2AlC and Ti_2AlN, indicating that Al_5C_3N is a ductile ceramic.

Keywords: electronic structure, chemical bonding, elastic properties, ductility

PACS: 62.20.de, 62.20.–x, 71.20.–b **DOI:** 10.1088/1674-1056/20/12/126201

1. Introduction

Recently, a class of ternary carbides and nitrides with layer-interleaved structure, called MAX phase or MAX-like compound, have generated increasing interest among researchers.[1−3] These compounds each have a unique combination of properties usually associated with metals and ceramics, including high Young's modulus, high electrical conductivity, high thermal conductivity, pseudoductility at room temperature, good resistance to high-temperature oxidation and thermal shock, and good tolerance to damage.[1] The aluminum-containing MAX(-like) ceramics, such as Ti_3AlC_2, Ti_2AlC, Cr_2AlC, Nb_2AlC, etc.[4−6] and Zr–Al–C ternary compounds[7−10] have been experimentally and theoretically studied in detail. The experimental results and the theoretical calculations indicated that the amazing properties resulted from the nano-laminated structure and weak bonding between different layers in the unit cell. This correlation provides a new route to the design of new structural materials with good mechanical properties similar to those of the MAX phases.

In the present work, we investigate the electronic band structures, the equation of state (EOS), and the mechanical properties of Al_5C_3N with the first-principles calculations, which have been used to obtain reliable elastic properties of inorganic carbides and nitrides.[11−13] In the Al–C–N system, four compounds, expressed stoichiometrically as a general formula $(AlN)_nAl_4C_3$, where $n = 1$ to 4, are clarified. The two members with n being odd numbers of 1 and 3 respectively of these four compounds, i.e., Al_5C_3N and $Al_7C_3N_3$, have space group symmetry $P6_3mc$ with two formula units per cell. The other two compounds with n being even numbers of 2 and 4 respectively, i.e., $Al_6C_3N_2$ and $Al_8C_3N_4$, have space group symmetry $R3m$ with one formula unit per cell. The structures of $(AlN)_nAl_4C_3$ have been discussed in detail by Jeffrey and Wu,[14] but the synthesis and properties of these aluminum carbonitrides have not been systematically reported to date. Our aim is to clarify the electronic properties, predict the physical properties, and provide a starting point for the research of $(AlN)_nAl_4C_3$ ceramics.

2. Crystal structure and computational detail

Figure 1 shows the crystal structure of Al_5C_3N. The lattice parameter a is 3.281 nm, and c is 21.670 nm. The atomic configuration of this compound can be described as an intergrown structure consisting of two kinds of tetrahedrons. One is the

*Project supported by the National Natural Science Foundation of China (Grant No. 10974041) and the Key Project of Science and Technology for Colleges in Hebei Province, China (Grant No. ZD2010120).

†Corresponding author. E-mail: tangcc@hebut.edu.cn

© 2011 Chinese Physical Society and IOP Publishing Ltd

hexagonal AlN slab and the other consists of Al and C atoms in an arrangement similar to that of binary aluminum carbide, Al_4C_3. In Al_5C_3N, three layers of point-shared AlC_x tetrahedron slabs are interleaved by the slab of AlN tetrahedron. Due to the different coordination environments, five kinds of aluminum atoms, three kinds of carbon atoms, and one nitrogen atom are distinguished and indexed with various numbers as shown in Fig. 1.

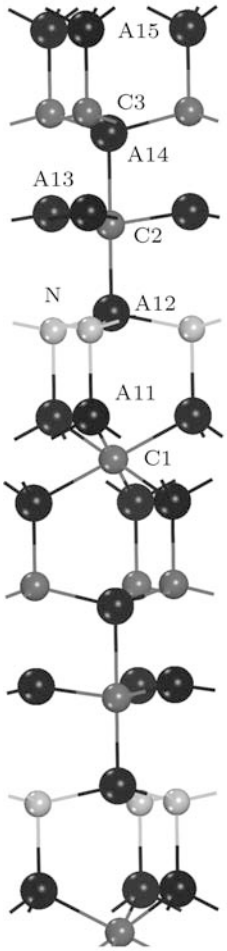


Fig. 1. Crystal structure of Al_5C_3N with the space group of $P6_3mc$ (Al: black ball; C: dark grey ball; N: light grey ball).

The *ab initio* calculations on ground-state electronic properties and EOS of Al_5C_3N were carried out in the framework of a plane-wave pseudopotential total energy method based on the density functional theory (DFT).[15,16] The plane-wave basis set cut-off energy was selected as 500 eV for all calculations, which was enough to lead a good convergence. The exchange–correlation energy of the electron–electron was treated under the generalized gradient approximation (GGA-PBE) scheme.[17] The special point sampling integration over Brillouin zone (BZ) was performed with 9×9×2 k-points meshes via the Monkhorst–Pack method.[18] The tolerances for the geometry optimization were selected as the difference in total energy within 1×10^{-6} eV/atom, the maximum ionic Hellmann–Feynman force within 2×10^{-3} eV/Å (1 Å=0.1 nm), the maximum stress of 4×10^{-3} GPa, and the maximum ionic displacement within 1×10^{-4} Å. The 20-percent empty bands were adopted, and the smearing energy was selected to be 0.05 eV. The optimized lattice parameters were in satisfactory agreement with the experimental values. The differences in lattice constant were less than 0.7%, which partially indicates that the calculated results are creditable. To investigate the mechanical properties of Al_5C_3N, we also optimized the geometric structure of the unit cell under the isostatic stress in a range of 11 GPa–70 GPa with the same tolerances setting.

3. Results and discussion

To illustrate the chemical bond characteristics of Al_5C_3N, the partial density of states (PDOS) of each element that is broken up into sites and the angular momentum contribution are also investigated, together with the total density of states, which are presented in Fig. 2. The band structure of Al_5C_3N is composed of two groups of valence bands and one group of conduction bands. An indirect gap, $\sim$ 0.81 eV, between valence bands and conduction bands, indicates that Al_5C_3N is a narrow-gap semiconductor, though the gap calculated with the density function theory (DFT) is usually lower than the experimental result.[19] For Al_5C_3N, the lower states lying around -16.0 eV and -14.1 eV originate mainly from the N 2s and C1 2s orbitals, respectively. Overlappings of Al4 2p and C2 2s orbitals, Al4 2p and C3 2s orbitals, Al3 2p and C2 2s orbitals extend from -13.1 eV to -9.8 eV. From -8.3 eV to the Fermi level (E_F), the valence bands contain strong sp-derived and pp-derived hybridization states of Al and C, Al and N, which make Al_5C_3N stable. The Al 3s–N 2p and the Al2 3s–N 2p covalent bonding states are located around -7.5 eV and -6.5 eV, respectively. The band of pp-derived hybridization states of Al2 and N atoms is composed of three peaks located at -6.6, -4.8, and -3.7 eV, respectively. While the Al 3p–C 2p covalent bonding states are located around -3.1, -1.8, and -1.2 eV respectively. Therefore, the chemical strength of the Al–C bond should be weaker than that of the Al–N bond.

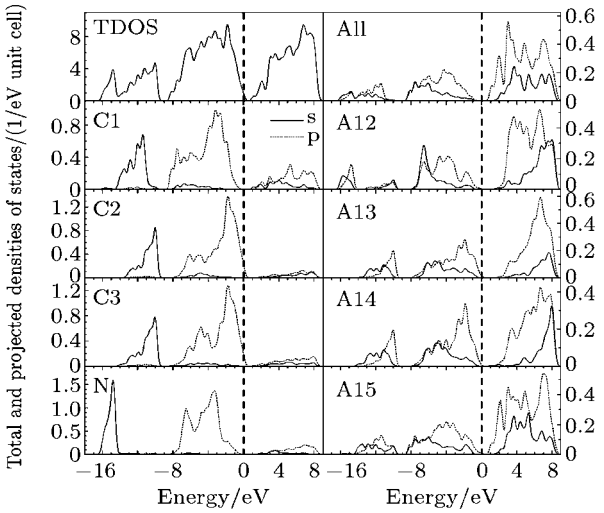


Fig. 2. Total and projected densities of states for Al_5C_3N each as a function of energy (E). The Fermi level is aligned with 0 eV.

Table 1 shows the Mulliken populations and lengths of bonds, and the charge of composed atoms in Al_5C_3N. Owing to the difference in electronegativity between the metallic and non-metallic atoms, the ionic bonds are formed since Al atoms donate some electrons to the non-metallic C and N atoms and thus become slightly positively charged. As mentioned above, the strong covalent bonds, derived from the sp and pp hybridizations, are formed between Al and C atoms, and Al and N atoms. The bonding nature can also be illustrated through the calculated total electron–charge–density contour as shown in Fig. 3. Due to the deviation of electron atmosphere and the charge transfer from Al to nonmetallic atoms, the charge-density around C and N atoms is the highest. The characteristic orbital of pp hybridization can be clearly observed between Al and C atoms, and between Al and N atoms in the calculated difference–electron–density counter plot. Note that the electron density between two Al–C–N slabs along the c axis is relatively low. Thus we suppose that the atomic chains of C1–Al1–N–Al2–C2–Al3(Al4)–C3–Al5 are formed in Al_5C_3N unit cells. A similar chain-like structure in Ti_3SiC_2 was also reported by Zhou *et al.*[20,21] So Al_5C_3N should have mechanical properties similar to those of MAX phases. However, dissimilar to the typical MAX phases with the metallic-covalent-ionic bonding, the chemical bond of Al_5C_3N can be characterized to be covalent-ionic. These bonds ought to be responsible for the significant anisotropies of thermal expansion and elastic constant, high modulus, and hardness.

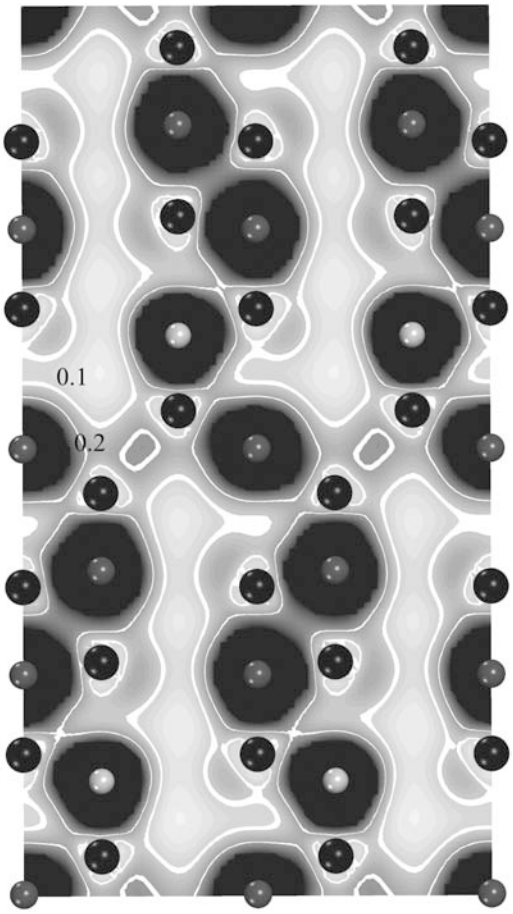


Fig. 3. Calculated total electrons–charge–density contour of $(11\bar{2}0)$ slice of Al_5C_3N 2×2×1 supercell.

Table 1. Calculated bond lengths and populations of various Al–C and Al–N bonds, and the charge number of various atoms in Al_5C_3N.

Bond	Bond length/Å	Bond population	Atoms	Charge/e
Al1–C1	2.0776	0.49	Al1	1.07
Al1–N	1.8092	0.40	Al2	1.27
Al2–N	1.9743	0.52	Al3	1.17
Al2–C2	1.9158	0.42	Al4	1.17
Al3–C2	1.8919	0.66	Al5	0.99
Al4–C2	2.1991	0.16	C1	–1.38
Al4–C3	1.9089	0.65	C2	–1.54
Al5–C3	1.8565	0.54	C3	–1.49
Al5–C1	2.1441	0.42	N	–1.27

Two methods are usually used to study the strengths of chemical bonds in compounds. One is to investigate the response of the bond under the external stress and the other is to calculate the bonding energy. We study the variation of length of the bonds between Al and nonmetallic atoms under different isostatic stresses in a range from 1 GPa to 70 GPa. The results show that the compressibilities of Al1–N, Al2–N, Al2–C2, and Al4–C2 bonds are higher than those of the other bonds. The bonding strength of these four weak bonds are also calculated from the following formula:

$$E_{\mathrm{A-B}} = [E_{\mathrm{AB}} - (E_{\mathrm{A-slab}} + E_{\mathrm{B-slab}})]/n, \quad (1)$$

where $E_{\mathrm{A-B}}$ is the bonding energy of A–B bond, E_{AB} is the total energy of AB unit cell, $E_{\mathrm{A-slab}}$ is the energy of the A slab after eliminating B slab in the unit cell, $E_{\mathrm{B-slab}}$ is the energy of the B slab after eliminating A slab, n is the number of molecules per unit cell. The calculated cohesive energies of Al1–N, Al2–N, Al2–C2, and Al4–C2 bonds are 0.89, 1.46, 0.98, and 0.76 eV, respectively. Therefore, Al_5C_3N can be described as the compound composed of Al_2C and Al_3C_2N slabs in structure.

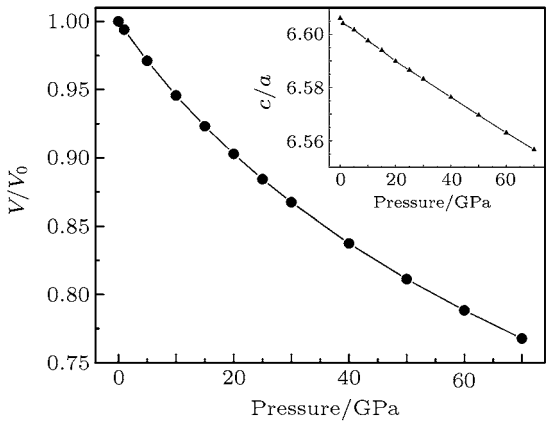


Fig. 4. Calculated pressure–volume relations for Al_5C_3N. The insert shows the pressure dependence of the relative lattice parameters (c/a) for Al_5C_3N.

The reliable elastic parameters can be obtained within a high accuracy by the *ab initio* calculation based on DFT. In this work, we adopted two methods to calculate the elastic properties of Al_5C_3N. One was the method to construct the equation of state (EOS), the other was the finite strain method. The geometry optimizations of Al_5C_3N were performed under the hydrostatic external pressure in a range from 1 GPa to 70 GPa. Figure 4 illustrates the dependences of cell volume and relative lattice constant (shown in the inset) on the external stress. It is indicated that no phase transformation occurs in the compressive procedure since the relative cell volume and lattice constant continuously decrease with the increase of pressure. Due to the bonding strength along the a axis of AlN and Al_4C_3 tetrahedrons in Al_5C_3N being close to that along the c axis, the relative lattice constant, c/a, decreases just by less than 1% as the pressure increases from 0 GPa to 70 GPa. According to a third order Birch–Murnaghan equation,[22] the bulk modulus at zero pressure B_0 and its pressure derivative B' are estimated as 195 GPa and 3.84 GPa, respectively.

Table 2 shows the stiffness constants, bulk modulus, shear modulus, Young's modulus, and Poisson's ratio of Al_5C_3N calculated with the second method mentioned above. For comparison, the corresponding constants of AlN, Al_4C_3[23], and several typical MAX ceramics[24–28] are also shown in the table. The stiffness constant is a proportional coefficient relating the given strain to the calculated stress by $\sigma_i = c_{ij}\varepsilon_j$.[29,30] Six different symmetry elements, including c_{11}, c_{12}, c_{13}, c_{33}, c_{44}, and c_{66}, can be resolved for a hexagonal crystal. The last component is not independent since $c_{66} = (c_{11} - c_{12})/2$. The bulk and shear moduli, B and G, can be computed by the following formulae suggested by Hill:[31]

$$B = \frac{1}{2}\left(B_{\mathrm{V}} + B_{\mathrm{R}}\right), \quad (2)$$

$$G = \frac{1}{2}\left(G_{\mathrm{V}} + G_{\mathrm{R}}\right), \quad (3)$$

where B_{V} and G_{V}, B_{R} and G_{R} are bulk and shear moduli deduced by Voigt and Reuss approximation, respectively. The dependences of these moduli on elastic coefficient in a hexagonal structure can be found elsewhere.[31,32] The correlations of Young's modulus E and Poisson's ratio ν of polycrystalline Al_5C_3N with B and G can be described with the following equations:

$$E = \frac{9BG}{3B+G}, \quad (4)$$

$$\nu = \frac{3B-2G}{2\left(3B+G\right)}. \quad (5)$$

For Al_5C_3N, the computed values of c_{11}, $(c_{11} - c_{12})$, c_{44}, and $(c_{11+}c_{12})c_{33} - 2c_{13}^2$ are positive, which is in accordance with the criteria of mechanical stability for a hexagonal crystal. The calculated c_{11} and c_{33}, associated with the principal stress–strain relation, are much higher than c_{44} and c_{66}, which are usually used to describe shear behaviours. And c_{11} is slightly less than c_{33}, implying that the bonding strengths along $[10\bar{1}0]$ and $[01\bar{1}0]$ directions are weaker than those along [0001] direction. The value of c_{44} is almost equal to that of c_{66}, implying that the shear behaviours along $[10\bar{1}0]$ (0001) are close to those along $[10\bar{1}0]$

$(01\bar{1}0)$. In a hexagonal structure, the anisotropic elastic behaviours can be described by three factors, related to the elastic coefficient as follows: $A_1 = 4c_{44}/(c_{11} + c_{33} - 2c_{13})$, $A_2 = 4c_{44}/(c_{22} + c_{33} - 2c_{23})$, and $A_3 = 4c_{66}/(c_{11} + c_{22} - 2c_{12})$, which are corresponding to $\{10\bar{1}0\}$, $\{01\bar{1}0\}$, and $\{0001\}$ shear planes along different directions, respectively. The computed values of A_1 and A_2 are both 0.64 and A_3 is 1, indicating that the $\{0001\}$ plane exhibits isotropy, while the other two planes deviate from isotropy. We also calculated the factor β, defined as the ratio of linear bulk modulus along the a axis to that along c axis, i.e., $\beta = (c_{11} + c_{12} - 2c_{13})/(c_{33} - c_{13})$.[33] The value of β is just about 1, implying the isotropy of elastic behaviour along different crystal axes, which is also mentioned above.

Table 2. Calculated values of elastic constant c_{ij} (GPa) and calculated bulk modulus B (GPa), shear modulus G (GPa), Young's modulus E (GPa), and Poisson's ratio υ of Al_5C_3N and relevant ceramics.

Compounds	c_{11}	c_{12}	c_{13}	c_{33}	c_{44}	c_{66}	B	G	E	υ
Al_5C_3N	374	158	82	421	101	108	201	116	292	0.26
Al_4C_3	352	115	52	391	116	119	170	129	309	0.20
AlN	382	130	105	352	114	126	199	122	304	0.25
Ti_3SiC_2	365	125	120	375	122	120	204	123	307	0.25
Ti_2AlC	321	76	100	318	144	123	166	128	305	0.19
Cr_2AlC	396	117	156	382	173	140	226	118	358	0.24
Ti_2AlN	309	66	91	280	125	122	155	118	281	0.20

The bulk modulus of Al_5C_3N, estimated from the finite strain method, is in good agreement with that calculated from the EOS. The calculated bulk and Young's moduli are slightly less than those of Ti_3SiC_2[24] and are higher than those of Ti_2AlC,[25,26] while the shear modulus of Al_5C_3N is almost equal to that of Ti_2AlC, and less than that of Ti_3SiC_2 (as shown in Table 1). The calculated B, G, E, and ν of Al_5C_3N are close to those of AlN in comparison with Al_4C_3. Pugh suggested that the ductility be defined as the ratio of bulk-to-shear-modulus, B/G.[34] Sun *et al.*[27] discussed the machinability of M_2AN represented with the ratio of bulk-modulus-to-c_{44}, B/c_{44}. For example, diamond has B/G and B/c_{44} of 0.9 and 0.8, and the corresponding values of Al, a typical metal, are 3.0 and 2.6, respectively.[35] The calculated ratios of bulk-to-shear-modulus and bulk-modulus-to-c_{44} of Al_5C_3N are 1.73 and 1.97, respectively, which are close to those of Cr_2AlN (B/c_{44} is about 2) and a bit higher than those of Ti_2AlC ($B/G = 1.29$ and $B/c_{44} = 1.15$, respectively) and Ti_2AlN ($B/G = 1.31$ and $B/c_{44} = 1.24$, respectively).[27,28] Hence, the aluminum carbonitride with hexagonal crystal, Al_5C_3N, is rather ductile, which is similar to the typical MAX ceramics. The unique chain-like structure in the unit cell of Al_5C_3N is suggested to result in the good ductility.

4. Conclusions

We studied the electronic structure, the chemical bonding, and the elastic properties of Al_5C_3N with the *ab initio* calculations. The aluminum carbonitride studied in this work is a semiconductor. Due to the strong orbital hybridization and charge transfer from Al to nonmetallic atoms, the chemical bonding of this compound can be characterized to be covalent-ionic. The calculated bulk, shear, and Young's moduli are 201, 116, and 292 GPa, respectively. The ductility and the machinability of Al_5C_3N, defined as the ratio of bulk-to-shear-modulus and bulk-modulus-to-c_{44}, are better than those of typical MAX phase, which may be attributed to the chain structure in the Al_5C_3N unit cell. We hope that these calculated results can inspire further experimental and theoretical study on Al_5C_3N.

References

[1] Barsoum M W 2000 *Prog. Solids St. Chem.* **28** 201

[2] Barsoum M W and EI-Raghy T 1996 *J. Am. Cera. Soc.* **79** 1953

[3] Barsoum M W, Brodkio D and EI-Raghy T 1997 *Scripta Mater.* **36** 535

[4] Sun Z M, Music D, Ahuja R, Li S and Schneider J M 2004 *Phys. Rev.* B **70** 092102

[5] Sun Z M, Li S, Ahuja R and Schneider J M 2004 *Solid State Commun.* **129** 589

[6] Manoun B, Kulkarni S, Pathak N, Saxena S K, Amina S and Barsoum M W 2010 *J. Alloys Compd.* **505** 328

[7] Wang J Y, Zhou Y C, Lin Z J, Liao T and He L F 2006 *Phys. Rev.* B **73** 134107
[8] Wang J Y, Zhou Y C, Lin Z J and Liao T 2005 *Phys. Rev.* B **72** 052102
[9] Sugiura K, Iwata T, Yoshida H, Hashimoto S and Fukuda K 2008 *J. Solid State Chem.* **181** 2864
[10] Zhang J, Wang J Y and Zhou Y C 2011 *J. Mater. Res.* **26** 372
[11] Yang T X, Cheng Q, Xu H B and Wang Y X 2010 *Acta Phys. Sin.* **59** 4919 (in Chinese)
[12] Fan X J, Li M K, Li C B, Liu F Q and Yin D 2005 *Chin. Phys.* **14** 2287
[13] Chen H C and Yang L J 2011 *Acta Phys. Sin.* **60** 014207 (in Chinese)
[14] Jeffrey G A and Wu Y V 1966 *Acta Cryst.* **20** 538
[15] Kohn W and Sham L J 1965 *Phys. Rev.* **140** A1133
[16] Kohn W 1999 *Rev. Mod. Phys.* **71** 1253
[17] Perdew J P, Burke K and Ernzerhof M 1996 *Phys. Rev. Lett.* **77** 3865
[18] Monkhorst H J and Pack J D 1976 *Phys. Rev.* B **13** 5188
[19] Milman V and Warren M C 2001 *J. Phys.: Condens. Matter* **13** 241
[20] Zhou Y C, Wang X H, Sun Z M and Chen S Q 2001 *J. Mater. Chem.* **11** 2335
[21] Zhou Y C and Sun Z M 2000 *J. Phys.: Condens. Mater* **12** L457
[22] Birch F 1978 *J. Geophys. Res.* **83** 1257
[23] Liao T, Wang J Y and Zhou Y C 2006 *Phys. Rev.* B **74** 174112
[24] Holm B, Ahuja R and Johansson B 2001 *Appl. Phys. Lett.* **79** 1450
[25] Wang J Y and Zhou Y C 2004 *Phys. Rev.* B **69** 214111
[26] Wang J Y and Zhou Y C 2004 *J. Phys.: Condens. Matter* **16** 2819
[27] Sun Z M, Music D, Ahuja R and Schneider J M 2005 *Phys. Rev.* B **71** 193402
[28] Cover M F, Warschkow O, Bilek M M M and McKenzie D R 2008 *Adv. Eng. Mater.* **10** 935
[29] Ashcroft N W and Mermin N D 1976 *Solid State Physics* (Philadelphia: Saunders College)
[30] Nye J F 1957 *Physical Properties of Crystals* (Oxford: Arendon)
[31] Hill R 1952 *Proc. Phys. Soc.* A **65** 349
[32] Bouhemadou A and Khenta R 2007 *J. Appl. Phys.* **102** 043528
[33] Ravindran P, Fast L, Korzhavyi P A, Johansson B, Wills J and Eriksson O 1998 *J. Appl. Phys.* **84** 4891
[34] Pugh S F 1954 *Philos. Mag.* **45** 823
[35] Kittel C 1996 *Introduction to Solid State Physics* (New York: Wiley)